

Lyman break galaxies as young spheroids

A. C. S. Friaça¹ and R. J. Terlevich^{2,3}

¹*Instituto Astronômico e Geofísico, USP, Caixa Postal 3386, 01065-970 São Paulo, SP, Brazil*

²*Institute of Astronomy, Madingley Road, Cambridge CB3 0EZ, UK*

³*Visiting Professor at Instituto Nacional de Astrofísica, Óptica y Electrónica. Av. Luis Enrique Erro 1, Tonanzintla, Puebla, Mexico*

26 April 2018

ABSTRACT

We investigate the nature of Lyman break galaxies (LBGs) using a chemodynamical model for evolution of galaxies. Our models predict an early (the first Gyr) stage of intense star formation in the evolution of massive spheroids which could be identified to the LBGs, observed at redshift ~ 3 with strong ongoing star formation. In particular, we are successful in reproducing the properties of the LBG DSF 2237+116 C2 with a model describing a young $\sim L^*$ spheroid. The comparison of the predictions of our models with the observations gives support to the scenario in which LBGs are the progenitors of present-day massive spheroids, i.e. bulges of luminous early type spirals or luminous elliptical galaxies.

Key words: cosmology: observations – galaxies: elliptical – galaxies: evolution – galaxies: formation – galaxies: ISM – galaxies: starburst

1 INTRODUCTION

Colour selection techniques based on the Lyman limit break of the spectral energy distribution caused by neutral hydrogen absorption have been used for many years in surveys for distant QSOs (e.g. Warren et al. 1987). Guhathakurta et al. (1990) and Songaila, Cowie & Lilly (1990) used this method to set limits on the number of star-forming galaxies at $z \approx 3$ in faint galaxy samples. More recently, Steidel & Hamilton (1992, 1993) and Steidel, Hamilton & Pettini (1995), using this method, designed a broad band filter set (the U_nGR system), which allowed them to discover a widespread population of star forming galaxies at redshift $z \simeq 3$, the Lyman break galaxies (LBGs). Spectroscopic confirmation of their redshifts was first presented by Steidel et al. (1996), and WFPC2 images of select LBGs were published by Giavalisco, Steidel & Macchetto (1996).

An important recent advance in the study of LBGs was the availability of the first results from a program of near-infrared spectroscopy aimed at studying the familiar rest-frame optical emission lines from H II regions of LBGs (Pettini et al 1998b, hereafter P98). The program was successful in detecting Balmer and [O III] emission lines in five LBGs. The nebular luminosities imply star formation rates (SFRs) larger than those deduced from the UV continuum, which suggests significant dust reddening. In four LBGs the velocity dispersion of the emission lines is $\sigma_{em} \simeq 70 \text{ km s}^{-1}$, while the fifth system has $\sigma_{em} \simeq 200 \text{ km s}^{-1}$. The relative redshifts of interstellar absorption, nebular emission, and Lyman α emission lines differ by several hundred km s^{-1} , a similar effect to that found in nearby HII galaxies (Kunth

et al 1998) indicating that large-scale outflows may be a common characteristic of both starbursts and LBGs.

On the other hand, we have developed a chemodynamical model (Friaça & Terlevich 1994; Friaça & Terlevich 1998, hereafter FT) for formation and evolution of spheroids, which are suspect to be the $z = 0$ counterparts of LBGs (Steidel et al. 1996). Our chemodynamical model combines multi-zone chemical evolution with 1-D hydrodynamics to follow in detail the evolution and radial behaviour of gas and stars during the formation of an spheroid. The star formation and the subsequent stellar feedback regulate episodes of wind, outflow, and cooling flow. The knowledge of the radial gas flows in the galaxy allows us to trace metallicity gradients, and, in particular, the formation of a high-metallicity core in ellipticals. The first ~ 1 Gyr of our model galaxies shows striking similarities to the LBGs: intense star formation, compact morphology, the presence of outflows, and significant metal content. We now proceed to examine these similarities, and, in particular, to consider the implications of the recent near-infrared observations of P98. We demonstrate that our model supports the scenario in which LBGs are the progenitors of the present-day bright spheroids. In this paper, the SFRs, luminosities and sizes quoted by P98 are converted to the cosmology adopted here ($H_0 = 50 \text{ km s}^{-1} \text{ Mpc}^{-1}$, $q_0 = 0.5$).

arXiv:astro-ph/9901321v1 22 Jan 1999

2 LYMAN BREAK GALAXIES AS YOUNG SPHEROIDS

There are several evidences in favour of the LBGs being the high-redshift counterparts of the present-day spheroidal component of luminous galaxies (Steidel et al. 1996, Giavalisco et al. 1996): their comoving space density is at least 25 % of that of luminous ($L \geq L^*$) present-day galaxies; the widths of the UV interstellar absorption lines in their spectra imply velocity dispersions of 180–320 km s⁻¹, typical of the potential well depth of luminous spheroids; they have enough binding energy to remain relatively compact despite the very high SN rate implied by their SFRs. In addition, the population of LBGs shows strong clustering in concentrations which may be the precursors of the present rich clusters of galaxies at a time when they were beginning to decouple from the Hubble flow (Steidel et al. 1998). In the context of Cold Dark Matter models of structure formation, the LBGs must be associated with very large halos, of mass $\gtrsim 10^{12} M_\odot$, in order to have developed such strong clustering at $z \sim 3$.

Assuming a Salpeter IMF, P98 inferred from the emission Balmer lines values for the SFR (uncorrected for dust) of their LBGs in the range 19–210 $h_{50}^{-2} M_\odot \text{ yr}^{-1}$. These values are typically a factor of several larger than those deduced from the UV continuum and indicate that the correction for dust is typically 1-2 magnitudes at 1500 Å. Dickinson (1998), for a large sample of LBGs, deduced from the UV continuum SFRs in the range 3–60 $h_{50}^{-2} M_\odot \text{ yr}^{-1}$. Assuming a 1 Gyr old continuous star formation, he used the $G - \mathcal{R}$ colours to compute corrections for dust extinction to the SFR. With a Calzetti (1997) attenuation law, after correction for dust extinction, the SFR range becomes $\sim 3 - \sim 1500 M_\odot \text{ yr}^{-1}$. These levels of star formation are remarkably close to the values of the SFR exhibited in the early evolution of the chemodynamical models of FT.

FT built a sequence of chemodynamical models reproducing the main properties of elliptical galaxies. The calculations begin with a gaseous protogalaxy with initial baryonic mass M_G . Intense star formation during the early stages of the galaxy builds up the stellar body of the galaxy, and during the evolution of the galaxy, gas and stars exchange mass through star formation and stellar gas return. Owing to inflow and galactic wind episodes occurring during the galaxy evolution, its present stellar mass is $\sim 15 - 70\%$ higher than M_G . Gas and stars are embedded in a dark halo of core radius r_h and mass M_h (we set $M_h = 3M_G$). The models are characterised by M_G , r_h , and a star formation prescription. The SFR is given by a Schmidt law $\nu_{SF} \propto \rho^{n_{SF}}$ (ρ is the gas density and $\nu_{SF} = SFR/\rho$ is the specific SFR). Here we consider the standard star formation prescription of FT, in which the normalization of ν is $\nu_0 = 10 \text{ Gyr}^{-1}$ (in order to reproduce the suprasolar [Mg/Fe] ratio of giant ellipticals), $n_{SF} = 1/2$, and the stars form in a Salpeter IMF from 0.1 to 100 M_\odot . A more detailed account of the models can be found in FT. Figure 1 shows the evolution of the SFR for models with M_G in the range $5 \times 10^9 - 5 \times 10^{11} M_\odot$ ($r_h = 0.8 - 5 \text{ kpc}$). During the maximum of the SFR, the stellar velocities dispersions of these models, 55–220 km s⁻¹, bracket the $\sigma_{em} = 55 - 190 \text{ km s}^{-1}$ range of the P98's LBGs. The corresponding present-day (age of 13 Gyr) luminosities are $0.05L^* - 1.4L^*$ ($-M_B = 17.6 - 21.3$). For

our models, the typical range of SFR averaged over the first Gyr, 10–700 $M_\odot \text{ yr}^{-1}$, reproduces well the SFRs found for LBGs, deduced from both the Balmer lines and the UV continuum corrected for dust extinction. In addition, the SFR drops dramatically after 1.5-2 Gyr, and becomes below the lowest SFRs found for the LBGs. The similarity of the SFRs of our models to those of LBGs allows us to identify the LBGs to young ($\lesssim 1 - 2 \text{ Gyr}$) spheroids.

It is important to note that the moderately high SFRs of the LBGs seem to be difficult to conciliate with the predictions of the simplistic one-zone (or monolithic) models of formation of elliptical galaxies for supra- L^* systems. The monolithic models of formation of early-type galaxies have been worked out in the early 1970's (e.g. Larson 1975) and are successful at reproducing the supra-solar [Mg/Fe] of bright ellipticals (Matteucci & Tornambé 1987; Hamann & Ferland 1993), but the required short star formation time scale ($\sim 10^8 \text{ yr}$) implies extremely high SFRs during the formation of $L > L^*$ ellipticals. As a matter of fact, in the one-zone model, a gaseous protogalaxy with $5 \times 10^{10} M_\odot$, would have a peak SFR of $\sim 5000 M_\odot \text{ yr}^{-1}$, and a present-day $M_B = -21.1$. At least at redshift $3 \lesssim z \lesssim 3.5$, such SFR is excluded by the properties of the population of LBGs. By contrast, in the chemodynamical model, the metallicity and abundance ratios of the central region of the young elliptical are explained with no need for all the galaxy having a global starburst coordinated with the central starburst, which avoids the excessively high SFRs of the one-zone model. The most massive model here ($M_G = 5 \times 10^{11} M_\odot$; present-day $M_B = -21.3$) has a peak SFR of 1050 $M_\odot \text{ yr}^{-1}$, consistent, after correction for dust extinction, with the highest SFRs derived from the UV continuum of LBGs (Dickinson 1998). Note that, as we show below, because the observed rest-frame UV colours limit the amount of dust extinction to $\sim 3 \text{ mag}$ at most, we cannot evoke dust to hide a 5000 $M_\odot \text{ yr}^{-1}$ starburst as a LBG at $z \sim 3$.

HST optical imaging, which probes the rest frame UV between 1400 and 1900 Å, has revealed that the LBGs are generally compact, with a typical half-light radius of 1.4–2.1 $h_{50}^{-1} \text{ kpc}$ (Giavalisco et al. 1996). The observed LBGs do not seem to have disk morphology, with the exception of a few objects without central concentration. In addition, some objects have a light profile following a $r^{1/4}$ law over a large radial range, which supports the identification of LBGs to young spheroids. Near infrared imaging have yielded half-light radii in the range 1.7–2.3 $h_{50}^{-1} \text{ kpc}$ (P98). The similarity of the near-infrared sizes to those obtained by the HST suggests that the optical morphology follows the UV morphology. As shown in the next section, the compact appearance of the LBGs, both in the UV and in the optical, is reproduced by our young spheroid models.

Note that, due to the strong fading of surface brightness with redshift ($\propto (1+z)^{-4}$), the outer parts ($r \gtrsim 10 \text{ kpc}$) of the galaxy with milder star formation rates ($\nu_{SF} \sim 1 \text{ Gyr}^{-1}$ or less) would be missed in high redshift observations. The difficulty in observing the outer regions of the galaxy would only be compounded if there is some dust extinction. There is an analogy between the LBGs and nearby HII galaxies, in which we are observing only the brightest part of the galaxy, superposed on much more extended low surface brightness object, when deeper expositions are made available (Telles & Terlevich 1997; Telles, Melnick & Terlevich 1997). Addi-

tional support to the LBG-starburst connection comes from the fact that the LBGs in the P98 sample fall on the extrapolation to higher luminosities of the correlation $L_{H\beta} - \sigma$ found for local H II galaxies by Melnick, Terlevich, & Moles (1988) (Terlevich 1998).

3 DSF 2237+116 C2, A YOUNG $\sim L^*$ SPHEROID?

It is of interest to compare the predictions for our models with the observational data of DSF 2237+116 C2, the most massive LBG (the LBG with the largest σ_{em}) in the P92 sample. The properties of this object are successfully described by the fiducial model of FT ($M_G = 2 \times 10^{11} M_\odot$ and $r_h = 3.5$ kpc). Its present-day stellar mass, $2.4 \times 10^{11} M_\odot$, corresponds to $L_B = 0.7L^*$, which allows us to identify DSF 2237+116 C2 to an $\sim L^*$ spheroid seen during its early evolution, characterised by intense star formation. For the fiducial model, Figure 1 shows the evolution of the SFR within several radii. The initial stage of violent star formation lasts ~ 1 Gyr, and exhibits a maximum SFR of $\sim 500 M_\odot \text{ yr}^{-1}$ at 0.6 Gyr. After the galactic wind is established (at $t = 1.17$ Gyr), the SFR plummets and practically all star formation within 10 kpc is concentrated inside the inner kpc. The late central star formation, characterised by a moderate SFR ($\sim \text{few } M_\odot \text{ yr}^{-1}$), is fed by a cooling flow towards the galactic centre. The stagnation point separating the wind and the inflow moves inwards until it reaches the galactic core at $t = 1.8$ Gyr, when a total wind is present throughout the galaxy. After this time, indicating the end of the star-forming stage, only very small levels of star formation are present in the galaxy. The early stage of star formation during which the stellar body of the galaxy is formed (the stellar mass reaches 50% of its present value at $t = 3.9 \times 10^8$ yr), resembles the LBGs. The average SFR during the first Gyr, $328 M_\odot \text{ yr}^{-1}$, is very similar to the SFR of $210h_{50}^{-2} M_\odot \text{ yr}^{-1}$ of DSF 2237+116 C2 inferred from its $H\beta$ luminosity. In addition, the SFR is concentrated in the inner 2-3 kpc, which gives to our model galaxy the compact appearance typical of LBGs.

Figure 1 also shows L_{1500} , the luminosity at 1500 \AA , which allows a more direct comparison with the imaging data. Note that our models reproduce the compact appearance of LBG, the light being concentrated in the inner ~ 3 kpc until the maximum of the SFR and in the inner ~ 2 kpc after that time. The luminosities predicted during the first Gyr are around $3 \times 10^{42} \text{ erg s}^{-1} \text{ \AA}^{-1}$. This value is higher than the observed L_{1500} of $4.1 \times 10^{41} h_{50}^{-1} \text{ erg s}^{-1} \text{ \AA}^{-1}$ found for DSF 2237+116 C2. Note that the $\propto (1+z)^{-4}$ dimming of the surface brightness with the redshift makes it difficult to detect the outer regions of the galaxy. However, considering the UV emission inside a projected radius of 10 kpc, reduces only slightly the UV luminosity ($L_{1500}(r < 10 \text{ kpc}) = 2.5 \times 10^{42} \text{ erg s}^{-1} \text{ \AA}^{-1}$). On the other hand, a simple comparison between the SFR deduced from the $H\beta$ line, assuming that the extinction at the $H\beta$ is negligible, and the SFR deduced from the UV continuum, indicates for DSF 2237+116 C2 a correction factor for dust between 7 and 48 (P98). These very high correction factors should not be taken at face value, since this simplistic approach furnishes some unphysical results, such as nega-

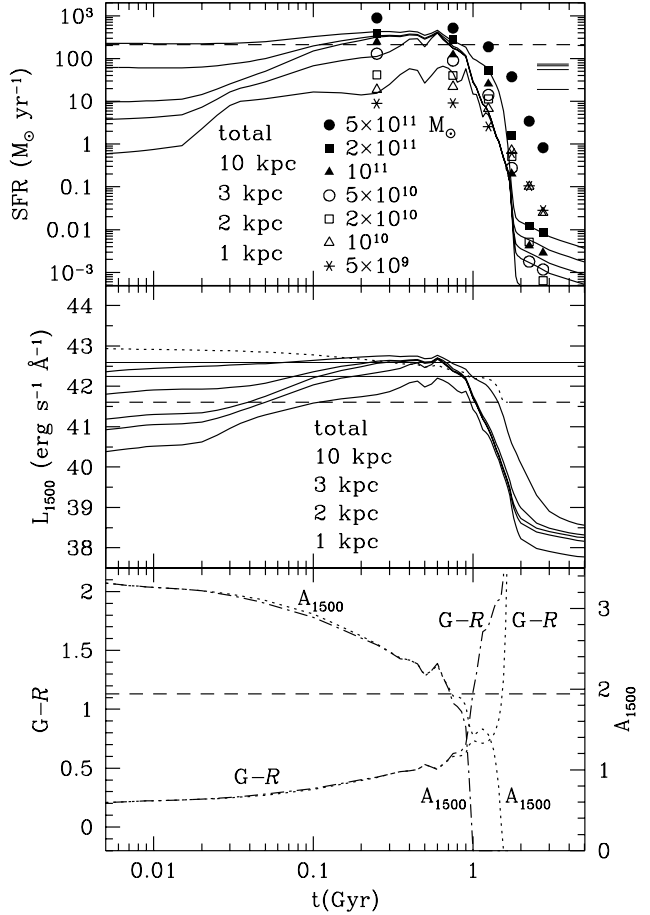


Figure 1. Top panel: evolution of the SFR for the fiducial over the whole galaxy and inside several radii. Also given the predicted SFRs averaged over the time spans 0-0.5, 0.5-1, 1-1.5, 1.5-2, 2-2.5, and 2.5-3 Gyr for several models (symbols labelled by the model M_G). Middle panel: evolution of the 1500 \AA luminosity over the whole galaxy and inside several projected radii. The luminosities have been calculated from the models of Bruzual & Charlot (1998), for a Salpeter IMF from 0.1 to $100 M_\odot$ and metallicities from $Z = 0.0001$ to $Z = 0.1$. Lower panel: evolution of the unreddened $G - R$ colour for the fiducial model, over the whole galaxy and inside a projected radius of 10 kpc (dotted and dot-dashed lines, respectively). Also shown (with the same line styles) the amount of reddening A_{1500} needed for $G - R$ of the model to match the observed $G - R$. In all three panels the dashed horizontal lines represent the respective observed quantities for DSF 2237+116 C2: SFR deduced from the $H\beta$ emission; L_{1500} uncorrected for dust; $G - R$ colour. In the middle panel, the two thin horizontal lines denote the observed L_{1500} with a correction for dust extinction deduced from the $G - R$ colour as in P98 (see text), and the dotted line indicates the observed L_{1500} corrected for dust extinction using the A_{1500} value over the whole galaxy shown in the lower panel. In the upper panel, the thin long dashes on the right denote the SFRs deduced from $H\beta$ emission for the $\sigma \approx 70 \text{ km s}^{-1}$ LBGs of P98; the highest value corresponds in fact to an upper limit for Q0000-263 D6, since for this object (at $z_{em} = 2.966$), $H\beta$ is outside the K-band, and the SFR was deduced from the $[\text{O III}]\lambda 5007$ luminosity, assuming $H\beta/[\text{O III}]\lambda 5007 \leq 0.5$.

tive extinctions for some objects. It would be interesting to consider a dust extinction index based on the UV part of the spectrum, the most easily accessible to observations of LBGs. The effect of dust is to flatten the spectrum, and the colour $G - \mathcal{R}$ provides a reliable measure of the UV slope (at $z \approx 3$, the effective redshifts of the two filters, 4740 and 6850 Å, respectively, are translated to 1190 and 1710 Å). The comparison of the observed $(G - \mathcal{R})_{obs}$ colours to the $(G - \mathcal{R})_{calc}$ colours predicted by an unreddened continuous star formation model with absorption by the Lyman α forest, allowed P98 to deduce dust correction factors between ~ 1 and ~ 10 for the UV luminosities of the LBGs in their sample. In the case of DSF 2237+116 C2, a value of $L_{1500} = 3.9(1.8) \times 10^{42} \text{ erg s}^{-1} \text{ \AA}^{-1}$ is obtained after a correction for dust extinction assuming a Calzetti attenuation law and a continuous $10^7(10^9)$ years old star formation.

In view of the importance of the $G - \mathcal{R}$ colour in checking for star formation and estimating the dust extinction, Figure 1 also shows $(G - \mathcal{R})_{calc}$ predicted for DSF 2237+116 C2 ($z = 3.317$) by the fiducial model, obtained as follows: in the first place, the integrated SED is calculated for several apertures, using the Bruzual & Charlot (1998) models; then the SED is redshifted to $z = 3.317$, reddened by the Lyman α forest opacity (Madau 1995), and convolved with the filter transmission curves. Finally, when $(G - \mathcal{R})_{calc}$ is bluer than the $G - \mathcal{R}$ colour of the galaxy ($(G - \mathcal{R})_{obs} = 1.13$), we calculate, assuming a Calzetti attenuation curve, the value of A_{1500} needed to match $(G - \mathcal{R})_{obs}$. Since $G - \mathcal{R}$ becomes redder with time, we can use the condition $(G - \mathcal{R})_{calc} < (G - \mathcal{R})_{obs}$ to set an upper limit in the age of the galaxy, beyond which A_{1500} becomes formally negative. This limit is 1.00 Gyr, for an aperture $r < 10$ kpc, and 1.52 Gyr, if the aperture encompasses the whole galaxy. The predicted colours are bluer for the larger aperture because: 1) metallicities are typically ~ 0.1 solar for $r > 10$ kpc, implying bluer colours for the star population; and 2) there is some star formation in the outer parts of the galaxy as the gas driven by the galactic wind is compressed on its way out of the galaxy. At the peak of the SFR, A_{1500} reaches ≈ 2.15 , within the range $A_{1500} = 1.58 - 2.44$ deduced by P98 for a continuous star formation lasting from 10^9 to 10^7 yr. Figure 1 also shows the observed value of L_{1500} corrected for dust extinction using the time-dependent value of A_{1500} obtained as above, and also the values corrected as in P98. The agreement with the predictions of our models both for the galaxy as a whole as for the inner 10 kpc is excellent. Therefore, if our model galaxy were at a redshift ~ 3 , it would be easily seen as an LBG.

In order to explore the recent availability of infrared imaging, tracing the rest-frame optical light, Figure 2 shows the blue luminosity of the fiducial model inside several projected radii. The similarity of rest-frame optical and UV sizes, indicated by the optical and near-infrared observations, is reproduced by the predictions of our model: the half-light radii at the maximum of SFR, at 1500 Å and in the blue band, are 1.64 and 1.51 kpc, respectively. It is useful, due to the possibility of missing light from the outer parts of the galaxy, to consider the half-light radii with respect only to the inner 10 kpc of the galaxy. In this case, the half-light radii at the SFR peak are 1.46 and 1.44 kpc, for 1500 Å and blue light, respectively. Therefore, the optical morphology follows the UV morphology, and the galaxy remains com-

pact in the optical band. Note, however, that the light *does not* trace the mass. At the maximum of SFR, the half-mass radius ($= 7.5$ kpc) is much larger than the half-light radius. The star formation does not follow the stellar mass, but instead it is regulated by the gas flows (e.g., the star formation within the inner kpc is fed by the cooling flow towards the galaxy centre). The star formation is not coordinated along the galaxy: ν_{SF} in the inner kpc reaches several $\times 10 \text{ Gyr}^{-1}$, whereas the ν_{SF} averaged over the whole galaxy is slightly larger than 1 Gyr^{-1} . In view of this, estimating the mass from the half-light radius will seriously underestimate the galaxy mass. P98 were suspicious of having underestimated the mass of DSF 2237+116 C2 (the value they derive is $5.5 \times 10^{10} M_{\odot}$). Here we quantify their suspicion, suggesting that the mass underestimate could be a factor 4-5. In fact, at the SFR peak, our model predicts not only half-light radii (whatever their definition) that are very similar to the $1.7h_{50}^{-1}$ found for DSF 2237+116 C2, but also a stellar velocity dispersion of 179 km s^{-1} , essentially identical to the observed $\sigma_{em} = 190 \pm 25$, whereas the stellar mass of our galaxy model is $2 \times 10^{11} M_{\odot}$ at this time.

The metal lines in the spectra of LBGs, with origin in stellar photospheres, interstellar absorption, and nebular emission, indicate metallicities anywhere between 0.01 solar and solar (Steidel et al. 1996). On the other hand, the strong correlation between the UV spectral index and metallicity in local starbursts would suggest a broad range in metallicity from substantially subsolar to solar or higher (Heckman et al. 1998). In order to make predictions on the metal content of LBGs, Figure 2 also shows the average metallicity of the stellar population, inside several spherical zones. The inner region reaches solar metallicities (at 1.11×10^8 and 1.56×10^8 for the inner kpc and for the $1 < r < 2$ kpc region, respectively) much earlier than the maximum in the SFR. Therefore, when the galaxy becomes visible as a LBG (i.e. as a star-forming galaxy), its metallicity inside a typical half-light radius (~ 1.5 kpc) will be solar or suprasolar. On the other hand, substantial abundance gradients are built up. The metallicity approaches $3 Z_{\odot}$ in the inner kpc, while it is typically $\sim 0.1 Z_{\odot}$ for $r > 10$ kpc.

Other important success of our models is the prediction of important outflows during the stage of intense star formation, which could account for the outflow at a velocity of $500 - 1000 \text{ km s}^{-1}$ in the interstellar medium of DSF 2237+116 C2 suggested by the relative velocities of the Lyman α emission lines and of the interstellar absorption lines. As a matter of fact, following the maximum of the SFR, an outflow appears at the intermediate radii, between 2 and 10 kpc. As we can see from Figure 2, once the outflow in the intermediate region is established, outflow flows velocities of $500 - 1000 \text{ km s}^{-1}$ are achieved for $t \sim 1$ Gyr. After 1.17 Gyr, when the outflow reaches the galaxy tidal radius (i.e. the onset of the galactic wind), the wind velocity increases up to about 1900 km s^{-1} . However, during the late galactic wind stage, the density in the outflowing gas drops dramatically, making it difficult to obtain any signature of the outflow via interstellar absorption lines and emission lines. The flow structure is complex, because at inner radii there is a highly subsonic (inflow velocity $\lesssim 10 \text{ km s}^{-1}$) cooling flow, and through the outer tidal there is infall of low density gas proceeding at 60 km s^{-1} . Therefore, the high density, high velocity outflowing gas in the intermediate region just after

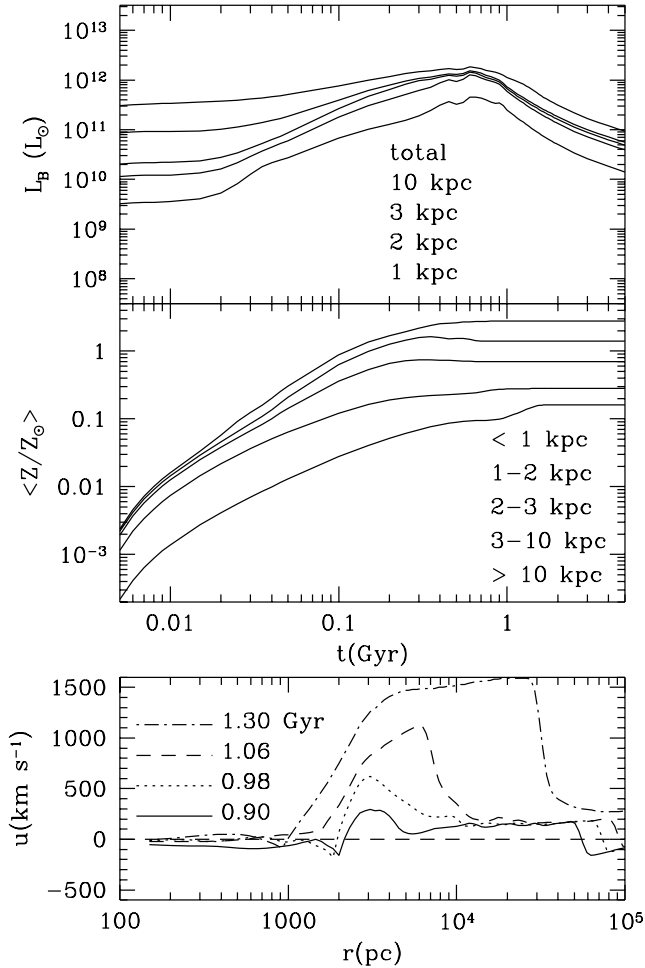


Figure 2. Top panel: evolution of the blue luminosity of the fiducial model inside several projected radii. Middle panel: evolution of the average metallicity of the stellar population, within several spherical zones, illustrating the presence of metallicity gradients and the time scales for chemical enrichment. The solar abundances are taken from Grevesse & Anders (1989). Lower panel: evolution of the velocity profile, showing the onset of the outflow at intermediate radii.

the peak in the SFR explains the large scale outflows with velocities of $\approx 500 \text{ km s}^{-1}$, deduced from the relative redshifts of the interstellar absorption and Lyman α emission lines, which are a common feature of LBGs (P98).

The success of our model for a $\sim L^*$ spheroid or elliptical galaxy in reproducing several properties of the LBG DSF 2237+116 C2 gives additional support to the scenario in which LBGs are the progenitors of present-day bright spheroids. High angular resolution spectroscopy will in the future provide important information regarding the velocity field and angular momentum of LBGs and help us to discern if they are young bulges or young ellipticals.

4 DISCUSSION

The agreement of the fiducial model with the properties of DSF2237-C2 suggests that the mass range of LBGs does include present day $\sim L^*$ objects. Note that the present model

not only accounts for this particularly massive LBG but also successfully predicts the properties of the ensemble of the LBGs, within the scenario in which they are the progenitors of the present day spheroids with $0.1L^* \lesssim L_B \lesssim L^*$. Our models also reproduce the main properties of the four LBGs with lower σ_{em} 's in P98. This is illustrated in Figure 1, in which the SFRs deduced for these LBGs are similar to those of models with $M_G = 10^{10} - 5 \times 10^{10} M_\odot$, for $t \lesssim 1 - 1.5$ Gyr (present day $-M_B = 18.4 - 19.7$).

These models chosen because they exhibit during the period $0.2 \leq t \leq 1.5$ Gyr (the lower limit on time guarantees that a significant stellar component has already been formed, and for times later than the upper limit, THE SFR has probably decreased below levels typical of LBGs) the stellar velocity dispersion coincides with the values of σ_{em} of the 4 low σ_{em} LBGs of P98 (which are in the range $55 \pm 15 - 85 \pm 15 \text{ km s}^{-1}$).

One of the central aspects of our modelling is that it follows in detail the impact of gas flows on the early evolution of the galaxies. Besides the importance of galactic winds in galaxy evolution, as already highlighted in the pioneering work of Larson (1974), cooling flows also play a central role in galaxy evolution — feeding a central AGN hosted in the galactic core, building up metallicity gradients (FT), and maintaining a moderate level of star formation in the inner regions of the galaxy at late times, i.e. when the major stellar population of the elliptical galaxy has already been formed (Jimenez et al. 1998).

As a matter of fact, the flow structure is complex, exhibiting, for instance, during a considerable span of the galaxy evolution a partial wind, with inflow in the inner parts of the galaxy and outflow in the outskirts of the galaxy.

Moreover, the flow structure varies with time, and the same star-forming galaxy can exhibit a variety of flow profiles, depending on the evolutionary stage being picked up by the observation. As can be seen from Figure 2, in the fiducial model the outflow does not occur during the whole period of intense star formation. Outflow velocities of $\sim 500 \text{ km s}^{-1}$ are achieved only ~ 0.3 Gyr after the maximum of the SFR and of $\sim 1000 \text{ km s}^{-1}$ ~ 0.4 Gyr after the maximum. The delay between the maximum of the SFR and the onset of the outflow reflects the time needed for the energy input by SNe into the ISM to overcome the gravitational binding energy of the gas. It is possible the observation of LBGs, i.e. with a high SFRs, in the phase of outflow and before the onset of the outflow. For earlier times, there are global inflows, reaching velocities of up to a few 100 km s^{-1} . Therefore, we expect a large dispersion in the relative redshifts of the interstellar absorption, nebular emission and Lyman α emission lines of LBGs. As we discuss below, this seems to be the case.

We can see from Figure 3 that for the models with M_G in the range $10^{10} - 5 \times 10^{10} M_\odot$, which describe well the four $\sigma_{em} \approx 70 \text{ km s}^{-1}$ in P98, the evolution of radial flows is qualitatively similar to that of the fiducial model. The main difference is that the outflow happens earlier, and, once the outflow is established, velocities higher than 1000 km s^{-1} are reached faster. This is a result of the shallower potential well of these galaxies. Note however, that the final wind velocities are somewhat lower than in the fiducial model.

Assuming that the Balmer and [O III] emission lines are at the galaxy systemic redshift, the velocity shifts of

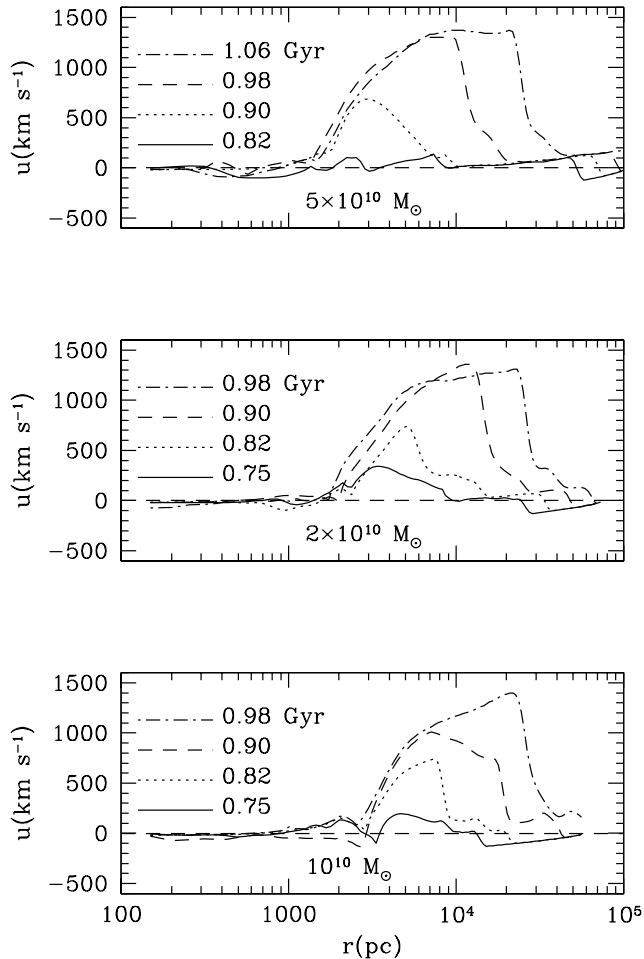


Figure 3. Evolution of the gas velocity profiles of low mass models aimed at describing the $\sigma \approx 70 \text{ km s}^{-1}$ galaxies of P98.

the interstellar absorption, nebular emission, and Lyman α emission lines found by P98 indicate that large velocity fields are a common feature of LBGs. It is important to note that exactly the same result has been found in nearby HII galaxies (Kunth et al. 1998). In all cases where Lyman α emission was detected, the line peak is shifted by $\approx 1000 \text{ km s}^{-1}$ relative to the metal absorption lines. In two out of three cases (Q0000–263 D6 and B2 0902+343 C6) the nebular lines are at intermediate velocities, with Q0000–263 D6 exhibiting a conspicuous P-Cygni profile. The most ready interpretation of these characteristics is the presence of large scale outflows with velocities of $\sim 500 \text{ km s}^{-1}$ in the interstellar media of the galaxies observed: the Lyman α emission is suppressed by resonant scattering and the only Lyman α photons escaping unabsorbed in our direction are those back-scattered from the far side of the expanding nebula, whereas in absorption against the stellar continuum we see the approaching part of the outflow. Within this scenario, the relative velocities of the three line sets of the LBGs are consistent with our model, since velocities of $\sim 500 \text{ km s}^{-1}$ are easily reached in the low mass models, at a galaxy age of 0.8–0.9 Gyr.

However, this simple symmetric picture probably does not account for all the variety of possible situations, since

in the third LBG with Lyman α emission (the high σ_{em} DSF 2237+116 C2) H β and [O III] emission are apparently at roughly the same velocity as the absorption lines, even though Lyman α emission is redshifted by $\approx 1000 \text{ km s}^{-1}$. Also this case could be explained by our models with the Lyman α emission originating in the high velocity shell receding in the back of the galaxy (in the fiducial model, at $t = 1.1 \text{ Gyr}$ this shell is at $r \approx 10 \text{ kpc}$ with a velocity of 1250 km s^{-1}), while the interstellar absorption lines could arise in the few central kpc, with much lower expansion velocities. See the interesting discussion regarding escape of Lyman α photons in HII galaxies by Kunth et al (1999).

In the P98 sample, 2 in 5 objects do not show Lyman α emission. In one of these systems (Q0201+113 B13) the interstellar absorption lines are *redshifted* by 250 km s^{-1} with respect to the H α emission (this object is at $z \approx 2.2$ and, as a consequence, H α is observed instead of H β). If this velocity difference is real (no error is quoted by P98 for the relative velocity of this object), within the scenario depicted by our model, we could be observing the galaxy during its early global inflow. The remaining object in P98 sample, also with no Lyman α emission, Q0201+113 C6, shows a 3200 km s^{-1} difference between emission and absorption lines, too large to be accounted for any for our models. As a matter of fact, this difference is so large that the line set identified as interstellar absorption could be in reality an intervening absorption line system. We would like to point that our predictions regarding the importance of the gas velocity field in the escape of Lyman α photons are similar to those of Kunth and collaborators for nearby HII galaxies (Kunth et al. 1998, 1999).

It is of interest to compare the results of the present model with the predictions for LBGs of the semi-analytic models of Baugh et al. (1998) and Mo, Mao, and White (1998) which are based on disk formation models. These models are simpler than the present model and, therefore, their predictions are more limited. For instance, Mo et al. (1998) do not discuss gas flows. However, in principle, their model could allow for some global characterization of the infall associated with the formation of a disk. Note that our prediction of outflows allows one to distinguish the present model from disk models, since disk models include infall but do not exhibit outflows.

One success of the models of Baugh et al. (1998) and Mo et al. (1998) is the good description of the clustering properties of the LBGs within the framework of the most popular hierarchical models for structure formation. Note these success refers in fact to the clustering of halos, independently if they host a spheroidal or a disklike star-forming central galaxy. Mo et al. (1998) claims to explain also the moderate SFRs, the small sizes and the velocity dispersions of the LBGs. However, as pointed out by Mo et al. themselves, their calculation of the SFR is very sketchy. In addition, their correct prediction of the compact size of the LBGs is a consequence of identifying the LBGs with low angular momentum objects, and so with small size for their mass. In connection to this last point, one of the parameters of the individual galaxies in Mo et al. (1998) is λ , the spin parameter of the halo, and for systems with λ smaller than some critical λ_{crit} , the gas cannot settle into a centrifugally supported disk without first becoming self-gravitating. The final configuration is probably spheroidal rather than disk-like.

In view of this, Mo et al. (1998) admits that a sizeable fraction of LBGs could be spheroids (see their Section 3.7), although their model was initially designed for the formation of disks. It is possible the existence of a population of disk objects among the LBGs, although the morphological studies of LBGs suggest that disks are a minority in the LBG population. *HST* imaging (filters F606W to F814W, probing the rest frame UV range 1400 – 1900 Å) has shown that the LBGs do not seem to have disk morphology, with the exception of a few objects without central concentration, for which an exponential profile provides a good fit to their surface brightness distribution (Giavalisco et al. 1996). In addition, some objects have a light profile following a $r^{1/4}$ law over a large radial range. Near-infrared *HST* NICMOS imaging (sensitive to the rest-frame optical light) provides a similar picture (Giavalisco, private communication). Future imaging observations would be very useful to establish which fraction of the LBGs are disk-like systems.

With respect to the velocity dispersions of the LBGs, Mo et al. (1998) reproduces the median values of the LBGs, but runs into some problems with the $\sigma \approx 200$ km s⁻¹ of DSF 2237+116 C2. since their predicted stellar velocity dispersions are typically around 70 km s⁻¹ for their $\Omega_0 = 1$ cosmology and 120 km s⁻¹ for their $\Omega_0 = 0.3$ flat cosmology. In the distribution of velocity dispersions predicted by Mo et al. (their Figure 8), the highest velocity dispersion is ~ 170 km s⁻¹ for the $\Omega_0 = 1$ cosmology and, even for the $\Omega_0 = 0.3$ flat cosmology (which predicts higher velocity dispersions), values of $\sigma \approx 200$ km s⁻¹ are very rare.

One interesting possibility offered by our modelling of the $G - \mathcal{R}$ colors is obtaining constraints on the age of the LBGs within the scenario of the young spheroid model. One minimal constraint is that the galaxy could not be older than ~ 1.5 Gyr, otherwise $G - \mathcal{R}$ would be redder than the observed. If, in addition to that, we require that the SFRs predicted for our model be consistent with the SFR derived from the H β emission, $SFR_{H\beta}$, the age of the LBG is constrained to be not older than ~ 1 Gyr. In this case, the predicted values for A_{1500} , 2.9 – 1.5 (for t from 0.1 to 1 Gyr), are comparable to those obtained by P98, because the evolution of the SFR of the fiducial model, with the constraint $t \lesssim 1$ Gyr and the strong decrease of the SFR beyond this time, includes their simple models of continuous star formation lasting for 10^7 yrs and 10^9 yr. On the other hand, P98 estimated a value of $A_{1500} = 4.2$, from comparing the SFRs deduced from H β and UV luminosities, assuming a Calzetti attenuation law and continuous star formation for 10^9 yrs. This value would represent a discrepancy with the values of A_{1500} predicted by our models, were it not for the fact that the simple comparison of H β and UV luminosities could lead to unreliable estimates of A_{1500} , as illustrated by some unphysical results, e.g. negative extinctions found by P98 for some objects. In determining A_{1500} from the $SFR_{H\beta}/SFR_{UV}$ ratio, one should be aware of the uncertainties in converting L_{1500} to SFR and that the long wavelength baseline involved in this estimation increases the uncertainties of assuming one particular extinction law.

Finally, the relatively high metal abundances obtained by our models, could be expected with some hindsight, if we had considered the high star formation rates derived for the LBGs, together with the continued (for periods ~ 1 Gyr

long) star formation favoured in previous works (e.g. Steidel et al. 1996). One of the important consequences of these relatively high metallicities coupled to the large outflow velocities is that the halo of the galaxy will be enriched in metals in $\sim 10^8$ yr, and the circumgalactic environment out to distances of several hundreds of kpc of the galaxy will be contaminated in metals in ~ 1 Gyr or less. This fast chemical enrichment mechanism for the galactic halo and in intergalactic medium could explain the chemical abundances of quasar absorption line systems, taken as a probe of the gaseous galactic halo and of the intergalactic medium as for instance, in Lyman limit systems (Viegas & Friaça 1995) and in the Lyman α forest (Friaça, Viegas & Gruenwald 1998).

ACKNOWLEDGMENTS

We thank Gustavo Bruzual for making us available the GISSEL code for evolutionary stellar population synthesis. We thank Mauro Giavalisco for supplying us with the filter transmission curves of the U_nGR system. A.C.S.F. acknowledges support from the Brazilian agencies FAPESP, CNPq, and FINEP/PRONEX. We would like to thank the anonymous referee, whose suggestions greatly improved this paper.

REFERENCES

- Baugh C.M., Cole S., Frenk C.S., Lacey C.G., 1998, ApJ, 498, 504
- Boyle B.J., Terlevich R.J., 1998, MNRAS, 293, L49
- Bruzual G., Charlot S., 1998, in preparation
- Calzetti D. 1997, in W.H. Waller, M.N. Fanelli, J.E. Hollis, A.C. Danks, eds, The Ultraviolet Universe at Low and High Redshift: Probing the Progress of Galaxy Evolution, AIP Conference Proceedings 408. Woodbury, New York, p. 40
- Dickinson M., 1998 in Livio M., Fall S.M., Mada P., eds, Proceedings of the STScI Symposium “The Hubble Deep Field”
- Friaça A.C.S., Terlevich R.J., 1994, in Tenorio-Tagle G., ed., Violent Star Formation from 30 Doradus to QSOs. CUP, Cambridge, p.424
- Friaça A.C.S., Terlevich R.J., 1998, MNRAS, 298, 399
- Friaça A.C.S., Viegas S.M., Gruenwald R., 1998, in P. Petitjean, S. Charlot, eds, Structure and Evolution of the Intergalactic Medium from QSO Absorption Line Systems. Editions Frontières, Paris, p. 406
- Giavalisco M., Steidel C.C., Macchetto F.D., 1996, ApJ, 470, 189
- Grevesse N., Anders E., 1989, in Waddington C.J., ed., Cosmic Abundances of Matter. AIP, New York, p.183
- Guhathakurta P., Tyson J.A., Majewski S.R., 1990, ApJ, 357, L9.
- Hamann F., Ferland G., 1993, ApJ, 418, 11
- Heckman T.M., Robert C., Leitherer C., Granett D.R., van der Rydt F., 1998, astro-ph/9803185
- Jimenez R., Friaça A.C.S., Dunlop J.S., Terlevich R., Peacock J.A., Nolan L.A., 1998, MNRAS, submitted
- Kunth, D., Mas-Hesse J.M., Terlevich E., Terlevich R., Lequeux, J., Fall, S.M., 1998, A&A, 334, 11
- Kunth, D., Terlevich E., Terlevich R., Tenorio-Tagle G., 1999, in Thuan T., Balkowski C., Cayette V., V&N J.T.T., eds, Proceedings of the XVIIIth Moriond Astrophysics Meeting on Dwarf Galaxies and Cosmology. Editions Frontières, Paris, in press. astro-ph/9809096
- Larson R.B., 1974, MNRAS, 169, 229
- Larson R.B., 1975, MNRAS, 173, 671
- Lowenthal J. et al., 1997, ApJ, 481, 673
- Madau P., 1995, ApJ, 441, 18

- Matsushita K., et al., 1994, *ApJ*, 436, L41
Matteucci F., Tornambè A., 1987, *A&A*, 185, 51
Melnick J., Terlevich R., Moles M. 1988, *MNRAS*, 235, 297
Mo H.J., Mao S., White S.D.M., 1998, *MNRAS*, submitted, astro-ph/9807341
Pettini M., Steidel C.C., Adelberger K.L., Kellogg M. Dickinson M., Giavalisco M., 1998a, in Shull J.M., Woodward C.E., Thronson H, eds., *ORIGINS. ASP Conf. Ser.*, in press
Pettini M., Kellogg M., Steidel C.C., Dickinson M., Adelberger K.L., Giavalisco M., 1998b, *ApJ*, in press (RGO pre-print No. 296; astro-ph/9806219)
Songaila A., Cowie L.L., Lilly S.J., 1990, *ApJ*, 348, 371
Steidel C.C., Hamilton D., 1992, *AJ*, 104, 941
Steidel C.C., Hamilton D., 1993, *AJ*, 105, 2017
Steidel C.C., Pettini M., Hamilton D. 1995, *AJ*, 110, 2519
Steidel C.C., Giavalisco M., Pettini M., Dickinson M., Adelberger K.L., 1996, *ApJ*, 462, L17
Steidel C.C., Adelberger K.L., Dickinson M., Giavalisco M., Pettini M., Kellogg M., 1998, *ApJ*, 492, 428
Telles, E. & Terlevich, R., 1997, *MNRAS*, 286, 183.
Telles, E., Melnick, J. & Terlevich, R., 1997, *MNRAS*, 288, 78.
Terlevich E., 1998, in the Proceedings of the La Plata meeting on “Massive stars”, in press
Terlevich R. J., Boyle B. J., 1993, *MNRAS*, 262, 491.
Viegas S.M., Friaça A.C.S., 1995, *MNRAS*, 217, L35
Warren S.J., Hewitt P.C., Irwin M.J., McMahon R.G., Bridgeland M.T., Bunclark P.S., Kibblewhite E.J., 1987, *Nature*, 325, 131.

This paper has been produced using the Royal Astronomical Society/Blackwell Science L^AT_EX style file.